Clim. Past Discuss., 10, 1305–1335, 2014
www.clim-past-discuss.net/10/1305/2014/
doi:10.5194/cpd-10-1305-2014

Climate of the Past
Discussions
Open Access

Variation in the Asian monsoon intensity and dry-wet condition since the Little Ice Age in central China revealed by an aragonite stalagmite

J.-J. Yin[1,2,3], D.-X. Yuan[1,2,3], H.-C. Li[1,2,4], H. Cheng[5,6], T.-Y. Li[3], R. L. Edwards[6], Y.-S. Lin[1,2], J.-M. Qin[1,2], W. Tang[1], Z.-Y. Zhao[3,7], and H.-S. Mii[8]

[1]Institute of Karst Geology, CAGS, Guilin, Guangxi 541004, China
[2]Key Laboratory of Karst Dynamics, MLR and Guangxi, Guilin, Guangxi 541004, China
[3]Key Laboratory of Eco-environments in Three Gorges Reservoir (Ministry of Education), School of Geographical Sciences, Southwest University, Chongqing 400715, China
[4]Department of Geosciences, National Taiwan University, Taipei 10617, Taiwan, Republic of China
[5]Institute of Global Environmental Change, Xi'an Jiaotong University, Xi'an 710049, China
[6]Department of Earth Sciences, University of Minnesota, Minneapolis 55455, USA
[7]Department of Environmental and Resource Sciences, LiuPanShui Normal University, Liupanshui 553004, China
[8]Department of Earth Sciences, National Taiwan Normal University, Taipei 11677, Republic of China

Received: 28 February 2014 – Accepted: 16 March 2014 – Published: 3 April 2014

Correspondence to: H.-C. Li (hcli1960@ntu.edu.tw)

Published by Copernicus Publications on behalf of the European Geosciences Union.

Abstract

Highlight: this paper focuses on the climate variability in central China since 1300 AD, involving:

1. A well-dated, 1.5 year resolution stalagmite δ^{18}O record from Lianhua Cave, central China;
2. Links of the δ^{18}O record with regional dry-wet condition, monsoon intensity, and temperature over eastern China;
3. Correlations among drought events in the Lianhua record, solar irradiation, and ENSO index.

We present a highly precisely ^{230}Th/U dated, 1.5 year resolution δ^{18}O record of an aragonite stalagmite (LHD1) collected from Lianhua Cave in Wuling mountain area of central China. The comparison of the δ^{18}O record with the local instrumental record and historical documents exhibits at least 15 drought events in the Wuling mountain and adjacent areas during the Little Ice Age, in which some of them were corresponding to megadrought events in the broad Asian monsoonal region of China. Thus, the stalagmite δ^{18}O record reveals variations in the summer monsoon precipitation and dry-wet condition in Wuling mountain area. The eastern China temperature varied with the solar activity, showing higher temperature under stronger solar irradiation which produces stronger summer monsoon. During Maunder, Dalton and 1900 sunspot minima, more severe drought events occurred, indicating weakening of the summer monsoon when solar activity decreased on decadal time scales. On interannual time scale, dry conditions in the studying area were prevailing under El Niño condition, which is also supported by the spectrum analysis. Hence, our record illustrates the linkage of Asian summer monsoon precipitation to solar irradiation and ENSO: wetter condition under stronger summer monsoon during warm periods and vice versa; During cold periods, the Walker circulation will shift toward central Pacific under El Niño condition, resulting further weakening of Asian summer monsoon. However, the δ^{18}O of LHD1 record is

CPD
10, 1305–1335, 2014

Little Ice Age in central China

J.-J. Yin et al.

positively correlated with temperature after ~1940 AD which is opposite to the δ^{18}O – temperature relationship in earlier time. This anomaly relationship might be caused by the greenhouse-gas forcing.

1 Introduction

The Little Ice Age (LIA, according to Matthes (1939) and Lamb (1977) from ~1550 AD to 1850 AD) was the last drift-ice cycle (Bond et al., 2001) characterized by cold conditions (PAGE 2k Consortium, 2013). Due to lower temperature in Northern Hemisphere during the LIA, the thermal equator and the rainy belt shifted southward (Broecker and Putnam, 2013), resulting in a drier condition in the Asian monsoon region (Wang et al., 2005; Zhang et al., 2008; Hu et al., 2008; Cui et al., 2012). Conversely, with the current warming, the rainy belt may presumably migrate northward and the monsoonal Asia would in turn become wetter (Broecker and Putnam, 2013). However, several high-resolution and precisely dated speleothem records in the Asian monsoon region (i.e., Zhang et al., 2008; Tan et al., 2009; Burns et al., 2002; Hu et al., 2008) reveal an excursion of the δ^{18}O toward heavier values over the past several decades that was interpreted as a weak monsoon trend. Therefore, the relationship between Asian summer monsoon precipitation and air temperature is not clear under the global warming trend. And, the driving force for variability of the Asian summer monsoon since the Little Ice Age is also unclear.

In this study, we establish a new high-resolution (~1.5 year) speleothem record from Lianhua cave, Hunan province, central China. Based on the record, we probe the relationships among solar irradiation, ENSO, temperature and summer monsoon precipitation and, in turn, the influencing factors for summer monsoon precipitation in eastern China since 1300 AD.

2 Cave site and local climate condition

Lianhua Cave (29°09′ N, 109°33′ E, 459 m a.s.l.) is located 36 km south of the Longshan City in the northwestern Hunan province of central China, and situated in the Wuling Mountain which is on the south bank of the middle Yangtze River between the Yunnan-Guizhou Plateau and Hunan Basin (Fig. 1). The host rock in the cave site is Upper Ordovician limestone enriched in dolomite. The main cave passage is about 580 m long connecting three main chambers (Fig. 2). The current entrance was found and enlarged during road construction in the late 20th century. In 2011, Stalagmite LHD1 was collected in the second chamber where abundant modern and fossil speleothems existed. The current cave temperature is about 16.3° with relative humid of > 95 %. Annual mean air temperature and rainfall at Longshan City in the instrumental records are 15.8° and ~ 1400 mm, respectively.

In northwest Hunan, about 77 % of annual precipitation falls in its rainy season between April and September (averaged from rainfall record of Yichang city between 1951 and 2012). After the rainy season, the rainy belt migrates to South China and precipitation decreases accordingly in the cave site. The oxygen isotope ($\delta^{18}O$) of precipitation becomes lighter during the rainy season, and reaches the lightest value in July and August (Liu et al., 2010, 2014; Cheng et al., 2012).

There are six meteorological stations around Lianhua cave, i.e., Youyang, Sangzhi, Longshan, Laifeng, Enshi and Yichang stations (Fig. 3). Precipitation records from these stations show essentially consistent variations in the past 60 years (Fig. 4), suggesting that the Lianhua Cave site may represent wet-dry condition of the entire Wuling Mountain area which is a function of the Asian summer monsoon variation and an indicator of regional flooding/drought events. In addition, note that the two precipitation plunges occurred during 1965–1966 and 1982–1983 when strong El Niño occurred.

CPD
10, 1305–1335, 2014

3 Sample, methods and results

3.1 Sample description

Stalagmite LHD1 is about 33 cm in height (Fig. 5). We halved the stalagmite along its growth axis. Its mineral composition and possible recrystallization were examined by using X-ray diffraction (XRD) on nine samples throughout the stalagmite in both the University of Science and Technology of China and the University of Minnesota, respectively. The XRD results indicate that the stalagmite is pure aragonite without recrystallization.

3.2 ^{230}Th/U dating and Chronology

A total of 25 subsamples with 10–100 mg in size for ^{230}Th dating were drilled along the growth axis at different depths, particularly at the top and bottom of each dark layer for potential hiatus. The chemical procedure used to separate uranium and thorium was following Edwards et al. (1987). U and Th measurements were made on Thermo Finnigan Neptune high precision multi-collector inductively coupled plasma mass spectrometer (MC-ICP-MS) in the Department of Earth Sciences, University of Minnesota (Cheng et al., 2013). Due to high U (1–6 ppm) and low ^{232}Th contents, the corrections of initial ^{230}Th and dating errors are very small (Table 1).

Based on the 25 ^{230}Th/U dates, stalagmite LHD1 grew continuously from 3290 ± 37 years BP to the present with an average growth rate of about 0.10 mm year^{-1}. Linear interpolation method is used to construct the age model (Fig. 5). The top 62 mm covers a time period from 1300 to 2011 AD, which includes the LIA and Current Warm Period (CWP). Except the top 0.5 mm, stable isotope resolution of the LHD1 record is about 1.5 years.

CPD
10, 1305–1335, 2014

3.3 $\delta^{18}O$ record

A total of 2995 subsamples for stable isotope analyses were drilled by using a computer-aided triaxial sampler with intervals of 0.1 mm after the first sample which contains the top 0.5 mm. Up-to-date, approximately 650 subsamples have been analyzed on Finnigan MAT-253 mass spectrometer equipped with a Kiel-III Carbonate Device in the Department of Geosciences at the National Taiwan University (NTU). The $\delta^{18}O$ values reported here are relative to the Vienna PeeDee Belemnite (VPDB) standard and the standard deviation of NBS-19 runs ($n = 358$) is better than 0.08 ‰. In order to make Hendy Test (Hendy, 1971), we took seven subsamples on each of the five layers at depths of 17.5, 86.5, 121, 192.5 and 264 mm by a hand driller. The seven sampling points are ~ 10 mm apart starting from the center. The 35 Hendy Test samples were measured by a GasBench III-Micromass IsoPrime IRMS in the Department of Earth Sciences at the National Taiwan Normal University.

Modern carbonate deposits and drip waters were collected during sampling of Stalagmite LHD1. The $\delta^{18}O$ value of drip water is −6.19 ‰ (VSMOW), and the $\delta^{18}O$ of modern speleothem deposit is −5.17 ‰ (VPDB). Using these values, we calculate depositional temperature under isotopic equilibrium using the following equation: $1000 \ln \alpha = 18.56(10^3/T) - 32.54$ (Thorrold et al., 1997). The calculated temperature is 15.7 °C which is similar to the measured cave temperature of 16.3 °C and the mean annual air temperature at the Longshan station.

Figure 6 shows our Hendy Test results. Although the $\delta^{18}O$ values along each layer exhibit significant variation, the center part has relatively constant $\delta^{18}O$ values. Within the sampling area (3 mm), the variations of the $\delta^{18}O$ are normally less than 0.05 ‰ (Fig. 6). For layers at 17.5 mm and 264 mm, there is no covariance between the $\delta^{18}O$ and $\delta^{13}C$. However, the $\delta^{18}O$ and $\delta^{13}C$ on layers at 86.5, 121 and 192.5 mm depths have apparent covariance. But, these correlations may be caused by age difference of the samples in the same layer rather than isotopic disequilibrium deposition. If the carbonate deposition was under significant evaporation, the $\delta^{18}O$ and $\delta^{13}C$ would be

CPD
10, 1305–1335, 2014

heavier on the edge of the stalagmite. In Fig. 6, no $\delta^{18}O$ trend is heavier toward the edges. In fact, it is impossible to drill samples on the same growth layer by hand and naked eye. Therefore, the Hendy Test shows no evidence of isotopic disequilibrium deposition. In addition, a few aragonite stalagmite records from Lianhua Cave had been published before (Cosford et al., 2008, 2009; Zhang et al., 2013), demonstrating that the aragonite stalagmites from the same cave had isotopic equilibrium.

The $\delta^{18}O$ values of the LHD1 record range from −5.04 to −6.75 ‰ (average −5.80 ‰) during the past 700 years and characterized by multi-decadal to centennial oscillations (Fig. 7). The average $\delta^{18}O$ value between 1300 and 1850 AD (in the LIA) is −5.82 ‰, actually undistinguishable from the average value of the whole record. In general, most $\delta^{18}O$ values during 1370–1590 AD were lighter than the average value. The $\delta^{18}O$ values between 1580 and 1850 AD which is the LIA were heavier than the average value, with the heavy values centered at 1640 AD, 1690 AD and 1780 AD. The $\delta^{18}O$ values between 1850 AD and 1950 AD were lighter than the average. Since 1950 AD, the $\delta^{18}O$ shifts toward heavy value and it reaches the heaviest value of −5.04 ‰ in the present (Fig. 7).

4 Discussion

4.1 Comparison of the $\delta^{18}O$ record with weather records

The link between cave $\delta^{18}O$ records and climate variation is in general complex as $\delta^{18}O$ of stalagmite is a function of cave temperature and $\delta^{18}O$ of dripping water which, in turn, is influenced by rainfall amount, air temperature, moisture source, summer/winter rain ratio, etc. (Wan et al., 2011). Changes in the summer monsoon intensity will affect all above factors (Li et al., 1998). Therefore, it is better to compare stalagmite $\delta^{18}O$ with the local instrumental weather records. In the Wuling Mountain and adjacent areas, precipitations are mostly affected by the Asian summer monsoon, and as aforementioned they show similar regional patterns (Fig. 4). Because of this reason, we select the Yichang rainfall record to compare with our Lianhua record, as this rainfall record is the longest (from 1882 to 2012 AD for precipitation and from 1905 to 2012 AD for temperature) (Fig. 8). In addition, a record of drought/wetness index since 1470 AD reconstructed from historic documents in this site exists (Fig. 7) (CAM, 1981; Zhang et al., 2003). Figure 8 shows that the Lianhua δ^{18}O record is comparable to the Yichang rainfall record before 1940: lighter δ^{18}O value corresponding to higher rainfall and vice versa, which can be explained by the "amount effect". Contrastingly, this relation broke after 1940. While δ^{18}O values in the Lianhua record show a dramatic increase trend towards today, the rainfall stays virtually at the same level (see later discussion). The correlation of the δ^{18}O record and rainfall record between 1910 and 1930 did not exist. This may be explained by the opposite direction of rainfall and temperature changes. This is because higher rainfall would result in lighter δ^{18}O, but colder temperature would lead to heavier δ^{18}O of carbonate precipitation (Fig. 8). The opposite effect of rainfall and temperature might obscure the "amount effect". In addition, δ^{18}O of rain in typical monsoonal area of China has negative correlation with air temperature (Johnson and Ingram, 2004; Li et al., 2007). In Fig. 8, the comparison between air temperature and the δ^{18}O record does not show any correlation except the opposite trend after 1980. Thus, one may accept that a heavy δ^{18}O execution in LHD1 record reflects drier condition under weak summer monsoon and colder temperature.

To further understand the Lianhua record beyond the instrumental record, we have compared the δ^{18}O record of LHD1 with a drought/flood index reconstructed from historic documents in Yichang area (Fig. 7). The historical record reveals 13 drought events, 1491–1493 (m), 1502 (l), 1585–1590 (k), 1616–1618 (j), 1637–1643 (i), 1689–1692 (h), 1729–1737 (g), 1756–1768 (f), 1784–1786 (e), 1856–1858 (d), 1876–1878 (c), 1886–1891 (b), and 1896–1903 (a), which can be seen in the δ^{18}O record of LHD1 (Fig. 7). Among those events, events (a), (b), (c), (d), (g), (h) and (i) affected more than 4 provinces with a duration of 3 years or more (Zhang, 2005); and events (c), (f), and (i) plus an event at 1790–1796 were reported previously as megadrought events in Asian monsoon region due to Asian summer monsoon failure (Cook et al., 2010).

Although the drought event (e) in the Yichang drought/flood index record is significant, it shows neither in the Lianhua record nor in any records in Asian monsoon region to our knowledge, perhaps due to a relatively local event occurred merely in Yichang area. In summary, it appears that the δ^{18}O record of LHD1 can be used as a rainfall proxy to indicate major drought events in the Asian monsoon region.

4.2 Solar radiation influence and teleconnection to ENSO

It has been well demonstrated that the Asian monsoon changes were dominantly controlled by Northern Hemisphere summer insolation on orbital timescale and the teleconnection with North Atlantic climate on millennial timescale (Wang et al., 2001, 2008; Cheng et al., 2009, 2012). However, the cause of the short-term drought events revealed in our Lianhua record was not clear. Therefore, we compare the δ^{18}O record of LHD1 with solar irradiation change (Fig. 9). Figure 9 exhibits that negative executions of δ^{18}O were generally corresponding to increase of solar irradiation, and more positive executions of δ^{18}O occurred during solar minima, including Spörer, Maunder, Dalton and 1900 minimum. This is because temperature change in eastern China was remarkably following the solar irradiation (Fig. 9). The correlation between the Lianhua δ^{18}O record and eastern China temperature (Wang et al., 2007; Shi et al., 2012) show a significantly negative correlation between 1548 and 1937 AD ($\delta^{18}\mathrm{O} = -6.20 - 1.307T$, $r^2 = 0.44$, $n = 253$). When solar irradiation decreased, temperature in eastern China became colder, which in turn led to weaker summer monsoon and resulted in heavier δ^{18}O in the stalagmite. Warmer condition under increased solar irradiation would enhance the summer monsoon and brought about wetter condition in the studying area.

However, solar irradiation (Delaygue and Bard, 2011) and temperature alone are difficult to explain all drought events in our record. For instance, during the periods of positive shifts (a), (b), (c) and (d) in the δ^{18}O of LHD1 record, solar irradiation and eastern China temperature did not show significant decrease (Fig. 9). Some other mechanisms must be involved. Comparison of our record to the El Niño 3.4 index (Cook, et al., 2008) shows that many drought events (positive executions of the δ^{18}O) occurred

CPD
10, 1305–1335, 2014

under the El Niño condition (Fig. 9), implying a possible linkage between the drought events and ENSO variations. During El Niño condition, the Walker Circulation shifted toward center Pacific, and sea surface temperature on the tropical western Pacific became cooler. Consequently, the East Asian summer monsoon could be weaker. Note that when solar irradiation was strong, the δ^{18}O became lighter even though during strong El Niño condition, e.g., during 1340 ~ 1400, 1720 ~ 1780 and 1920 ~ 1950 AD (Fig. 9). This means that under warm stages when the solar irradiation was strong, the effect of ENSO variation on the East Asian summer monsoon strength was small.

Power spectrum analysis (Schulz and Mudelsee, 2002) of the Lianhua δ^{18}O time series shows significant periodicities of 2.6–2.7 years (excess 95 % confidence levels), 3.4–4.1 years (excess 80 % confidence level) and 47 years (excess 95 % confidence levels) (Fig. 10). The periodicities of 2.7 and 4.1 year can be seen in the spectrum analysis of Niño 3.4 record (Fig. 10), and is considered as one periodicity of ENSO variability. The 47 year periodicity matches with the 44 year cycle of solar activity, which has also shown in other cave records in the Asian monsoon region, for example, in Dongge cave record (Dykoshi et al., 2005; Kelly et al., 2006) and Jiuxian cave record (Cai et al., 2010). These results from spectrum analysis support the link of Asian monsoon rainfall to solar activity and ENSO.

4.3 The relationship of δ^{18}O-temperature before and after 1940

It is a classic wisdom that high continental temperature will enhance land-sea thermal contrast and in turn intensify the summer monsoon (e.g., Kutzbach, 1981). Intensified summer monsoon may be associated with a stronger and larger atmospheric circulation that may transfer more remote moisture from the tropical oceans to the land, resulting lighter δ^{18}O of rainfall due to fractionation during moisture transportation (Cheng et al., 2012). In other words, the δ^{18}O of precipitation in eastern China is mainly modulated by the Asian summer monsoon system, and thus δ^{18}O of our stalagmite records indicate mainly integrated Asian monsoon intensity (Cheng et al., 2009, 2012; Liu et al., 2014).

CPD
10, 1305–1335, 2014

As we mentioned before, lighter $\delta^{18}O$ in the LHD1 record corresponds to higher temperature in eastern China before 1940, and vice versa (Fig. 9). However, this correlation did not appear in two periods: 1410–1530 AD and after 1940 AD (Fig. 9). During 1410–1530 AD, the eastern China temperature was low, corresponding to the Spörer solar minimum. For this period, the $\delta^{18}O$ record was influenced by ENSO condition, with lighter $\delta^{18}O$ corresponding to the La Niña condition and heavier $\delta^{18}O$ corresponding to the El Niño condition (Fig. 9). It is possible that the strong La Niña condition led to more moisture source from Indian Ocean which had lighter $\delta^{18}O$ to reach the studying area, instead of heavy rainfall. Therefore, solar activity, the monsoonal strength and ENSO condition of natural conditions all play important roles in the "amount effect" and moisture source effect on the stalagmite $\delta^{18}O$ on decadal-to-centennial scales. It seems that during cold stages, the influence of ENSO condition became dominant.

The strongly warming trend in eastern China temperature after ~ 1950 AD did not result in an increase of the summer monsoon strength, nor a depletion trend in the Lianhua $\delta^{18}O$ record (Fig. 9). In fact, many speleothem records in the Asian monsoonal region showed an enriched $\delta^{18}O$ trend after 1950 (Fig. 11). Zhang et al. (2008) explained this phenomenon as human impact on the temperature–monsoon relationship. Actually, the measured East Asia summer monsoon index had a decreasing trend since 1950 (Wang et al., 2006). Therefore, one can expect that the enriched speleothem $\delta^{18}O$ trend reflect the weakening the monsoon trend. However, how the anthropogenic forcing to break the natural relationship between the Asian monsoon and eastern China temperature needs to be understood. Model simulations have shown that anthropogenic black-carbon and/or sulfate-aerosol could reduce Asian monsoon rainfall (Bollasina et al., 2011). A recent modeling work has also demonstrated that temperature increase due to greenhouse gas increase may weaken, rather than enhance, the Asian monsoon (Liu et al., 2013). Another plausible explanation invokes the intensifying of the hydrological cycle and widening of the tropical belt due to greenhouse-gas forcing as suggested by recent studies (Marvel and Bonfils, 2013). All these results are consistent with our observation that suggests the Asian monsoon weakening during the past half century is likely caused by the greenhouse-gas forcing.

4.4 Comparison of speleothem records in the Asian monsoonal region

Since late 1990s, numerous speleothem records have been generated. On millennial to orbital scales, many speleothem records from the monsoonal regions are comparable as the dominant factors to influence the summer monsoon strength were changes in solar insolation and major ocean circulation. Although our study indicates that variations of solar irradiation, air temperature and ENSO condition are important forcing factors to influence the Asian monsoonal climates on decadal to centennial scales, whether speleothem records on such time scales are comparable remains question. Here we put some available high-resolution speleothem records from the Asian monsoonal regions together, including S3 record from Defore Cave in Oman (Burns et al., 2002), DA record from Dongge Cave (Wang et al., 2005), HS-4 record from Heshang Cave (Hu et al., 2008), DY-1 record from Dayu Cave (Tan et al., 2009), WX42B record from Wanxiang Cave (Zhang et al., 2008) and LHD1 record (this study) (Fig. 11). These records were well dated with age uncertainty generally less than 50 years. From the comparison in Fig. 11, it is difficult to see consistent trends either on decadal scale or centennial scale over entire eastern China. In fact, on annual-to-centennial scales, forcing factors of monsoonal variability are more and further complicated. Considering that the eastern China monsoonal region is a broad area with complicated geographical setting, the summer monsoon rain has strongly spatial disparity. In order to understand paleo-monsoonal climates over eastern China, more well-dated and high-resolution records from different locations need to be reconstructed.

CPD
10, 1305–1335, 2014

5 Conclusions

The well-dated, high-resolution δ^{18}O record of aragonite Stalagmite LHD1 from Lianhua Cave in Wuling mountain area, central China since 1300 AD has been compared with instrumental weather records, historic dry/wetness index, eastern China temperature, Solar irradiation and ENSO variation. The δ^{18}O record on decadal to centennial scales reflects mainly changes in local dry-wet condition which is tightly related to the summer monsoon intensity. Intensified summer monsoon under high continental temperature caused by enhanced solar irradiation will provide wetter condition in central China, resulting lighter δ^{18}O execution in LHD1 record. During cold stages, ENSO variation becomes a major factor to influence the East Asian summer monsoon, with weak summer monsoon under El Niño condition and strong monsoon under La Niña condition. Spectrum analysis of the LHD1 δ^{18}O record appears 2–4 years and 47 years cyclicities, indicating the summer monsoon intensity link to solar activity and ENSO variation. Before 1940, the LHD1 δ^{18}O record that is an indicator of the East Asian summer monsoon intensity had a negative correlation with the eastern China temperature. However, since ~1950 AD, this correlation has reversed, showing weakening summer monsoon intensity with increased temperature. Our record seems to support that greenhouse-gas forcing may play an important role in summer monsoon precipitation variations. On annual-to-centennial scales, speleothem δ^{18}O records over the monsoonal region cannot be consistent due to multiple forcing factors on the summer monsoon intensity, complicated geographical settings and regional disparity of monsoonal rain. One may not except to use single speleothem record to interpret monsoonal climates over the vest eastern China. The LHD1 δ^{18}O record shows that on centennial scales warmer and wetter conditions were prevailing during 1300 ~ 1550 AD and 1850 ~ 1950 AD in the Wuling Mountain area. During 1550 ~ 1850 AD of the LIA, climate in the Wuling Mountain area was cold and dry. On decadal scales, drought events occurred ca. 1350, 1420, 1450, 1500, 1550, 1590, 1620, 1640, 1690, 1735, 1760, 1785, 1855, 1877 and 1890 AD.

CPD
10, 1305–1335, 2014

Acknowledgements. This project was supported by grants from Geological survey program of Ministry of Land and Resource of China (Granted No. 12120113006700), China Scholar Council (Granted No. 201206990052), National Science Foundation of China (Granted No. 41072192). Grants from NSC101-2116-M-002-007 and 102-2811-M-002-177 to H.-C. Li supported stable isotope analyses. NSFC 41230524 to H. Cheng and NSFC (41172165) to T.-Y Li are also acknowledged. Thanks to Rich Knurr for the XRD analysis in Department of Earth Sciences at University of Minnesota. We also thank Yanbin Lu, Julie Retrum and Mellissa Cross for their help in U-Th dating in University of Minnesota. Aoyu Wang, Guangde Zhu and Guansheng Xiang are acknowledged for their help in field work.

References

Bollasina, M. A., Ming, Y., and Ramaswamy, V.: Anthropogenic aerosols and the weakening of the South Asian Summer Monsoon, Science, 334, 502–505, 2011.

Bond, G., Kromer, B., Beer, J., Muscheler, R., Evans, M. N., Showers, W., Hoffmann, S., Lotti-Bond, R., Hajdas, I., and Bonani, G.: Persistent solar influence on North Atlantic climate during the Holocene, Science, 294, 2130–2136, 2001.

Broecker, W. S. and Putnam, A. E.: Hydrologic impacts of past shifts of earth's thermal equator offer insight into those to be produced by fossil fuel CO_2, P. Natl. Acad. Sci. USA, 110, 16710–16715, 2013.

Burns, S. J., Fleitmann, D., Mudelsee, M., Neff, U., Matter, A., and Mangini, A.: A 780-year annually resolved record of Indian Ocean monsoon precipitation from a speleothem from south Oman, J. Geophys. Res., 107, 4434, doi:10.1029/2001JD001281, 2002.

Cai, Y., Tan, L., Cheng, H., An, Z., Edwards, R. L., Kelly, M. J., Kong, X., and Wang, X.: The variation of summer monsoon precipitation in central China since the last deglaciation, Earth Planet. Sc. Lett., 291, 21–31, 2010.

Cheng, H., Edwards, R. L., Broecker, W. S., Denton, G. H., Kong, X., Wang, Y., Zhang, R., and Wang, X.: Ice age terminations, Science, 326, 248–252, 2009.

Cheng, H., Sinha, A., Wang, X., Cruz, F. W., and Edwards, R. L.: The global paleomonsoon as seen through speleothem records from Asia and the Americas, Clim. Dynam., 39, 1045–1062, 2012.

CPD
10, 1305–1335, 2014

Little Ice Age in central China

J.-J. Yin et al.

Cheng, H., Edwards, R. L., Shen, C.-C., Polyak, V. J., Asmerom, Y., Woodhead, J., Hellstrom, J., Wang, Y., Kong, X., Spötl, C., Wang, X., and Alexander Jr., E. C.: Improvements in ^{230}Th dating, ^{230}Th and ^{234}U half-life values, and U-Th isotopic measurements by multi-collector inductively coupled plasma mass spectrometry, Earth Planet. Sc. Lett., 371–372, 82–91, 2013.

Chinese Academy of Meteorological Sciences (CAM): Yearly Charts of Dryness/Wetness in China for the Last 500-Year Period, Beijing, SinoMap Cartogr. Publ. House, Beijing, 1981 (in Chinese).

Cook, E. R., D'Arrigo, R. D., and Anchukaitis, K. J.: ENSO reconstructions from long tree-ring chronologies: unifying the differences, in: Talk presented at a special workshop on Reconciling ENSO Chronologies for the Past 500 Years, Moorea, French Polynesia, 2–3 April 2008, 2008.

Cook, E. R., Anchukaitis, K. J., Buckley, B. M., D'Arrigo, R. D., Jacoby, G. C., and Wright, W. E.: Asian monsoon failure and megadrought during the last millennium, Science, 328, 486–489, 2010.

Cosford, J., Qing, H., Eglington, B., Mattey, D., Yuan, D., Zhang, M., and Cheng, H.: East Asian monsoon variability since the Mid-Holocene recorded in a high-resolution, absolute-dated aragonite speleothem from eastern China, Earth Planet. Sc. Lett., 275, 296–307, 2008.

Cosford, J., Qing, H., Mattey, D., Eglington, B., and Zhang, M.: Climatic and local effects on stalagmite δ^{13}C values at Lianhua Cave, China, Palaeogeogr. Palaeocl., 280, 235–244, 2009.

Cui, Y. F., Wang, Y. J., Cheng, H., Zhao, K., and Kong, X. G.: Isotopic and lithologic variations of one precisely-dated stalagmite across the Medieval/LIA period from Heilong Cave, central China, Clim. Past, 8, 1541–1550, doi:10.5194/cp-8-1541-2012, 2012.

Delaygue, G. and Bard, E.: An Antarctic view of Beryllium-10 and solar activity for the past millennium, Clim. Dynam., 36, 2201–2218, 2011.

Dykoski, C. A., Edwards, R. L., Cheng, H., Yuan, D., Cai, Y., Zhang, M., Lin, Y., Qin, J., An, Z., and Revenaugh, J.: A high-resolution, absolute-dated Holocene and deglacial Asian monsoon record from Dongge Cave, China, Earth Planet. Sc. Lett., 233, 71–86, 2005.

Edwards, R. L., Chen, J. H., and Wasserburg, G. J.: ^{238}U-^{234}U-^{230}Th-^{232}Th systematics and the precise measurement of time over the past 500,000 years, Earth Planet. Sc. Lett., 81, 175–192, 1986.

CPD
10, 1305–1335, 2014

Little Ice Age in central China

J.-J. Yin et al.

Hendy, C. H.: The isotopic geochemistry of speleothems: 1. The calculation of the effects of different modes of formation on the isotopic composition of speleothems and their applicability as paleoclimatic indicators, Geochim. Cosmochim. Ac., 35, 801–824, 1971.

Hu, C., Henderson, G. M., Huang, J., Xie, S., Sun, Y., and Johnson, K. R.: Quantification of Holocene Asian monsoon rainfall from spatially separated cave records, Earth Planet. Sc. Lett., 266, 221–232, 2008.

Jaffey, A. H., Flynn, K. F., Glendenin, L. E., Bentley, W. C., and Essling, A. M.: Precision measurement of half-lives and specific activities of ^{235}U and ^{238}U, Phys. Rev. C, 4, 1889–1906, 1971.

Johnson, K. R. and Ingram, B. L.: Spatial and temporal variability in the stable isotope systematics of modern precipitation in China: implications for paleoclimate reconstructions, Earth Planet. Sc. Lett., 220, 365–377, 2004.

Kelly, M. J., Edwards, R. L., Cheng, H., Yuan, D., Cai, Y., Zhang, M., Lin, Y., and An, Z.: High resolution characterization of the Asian monsoon between 146,000 and 99,000 years B. P. from Dongge Cave, China and global correlation of events surrounding Termination II, Palaeogeogr. Palaeocl., 236, 20–38, 2006.

Kutzbach, J. E.: Monsoon climate of the early Holocene: climate experiment with the earth's orbital parameters for 9000 years ago, Science, 214, 59–61, 1981.

Lamb, H. H.: Climatic History and the Future, Princeton Univ. Press, Princeton, NJ, 835 pp., 1977.

Li, H.-C., Ku, T.-L., Stott, L. D., and Chen, W.-J.: Applications of interannual-resolution stable isotope records of speleothem: climatic changes in Beijing and Tianjin, China during the past 500 years – the δ^{18}O record, Sci. China Ser. D, 41, 362–368, 1998.

Li, H.-C., Yuan, D.-X., Ku, T.-L., Wan, N.-J., Ma, Z.-B., Zhang, P.-Z., Bar-Matthews, M., Ayalon, A., Liu, Z.-H., Zhang, M.-L., Zhu, Z.-Y., and Wang, R.-M.: Stable isotopic compositions of waters in the karst environments of China: climatic implications, Appl. Geochem., 22, 1748–1763, 2007.

Liu, J., Song, X., Yuan, G., Sun, X., Liu, X., and Wang, S.: Characteristics of δ^{18}O in precipitation over eastern monsoon China and the water vapor sources, Chinese Sci. Bull., 55, 200–211, 2010.

Liu, J., Wang, B., Cane, M. A., Yin, S.-Y., and Lee, J.-Y.: Divergent global precipitation changes induced by natural versus anthropogenic forcing, Nature, 493, 656–659, 2013.

Liu, Z., Wen, X., Brady, E. C., Otto-Bliesner, B., Yu, G., Lu, H., Cheng, H., Wang, Y., Zheng, W., Ding, Y., Edwards, R. L., Cheng, J., Liu, W., and Yang, H.: Chinese cave records and the East Asia Summer Monsoon, Quaternary Sci. Rev., 83, 115–128, 2014.

Marvel, K. and Bonfils, C.: Identifying external influences on global precipitation, P. Natl. Acad. Sci. USA, doi:10.1073/pnas.1314382110, in press, 2013.

Matthes, F. E.: Report of the committee on glaciers, EOS T. Am. Geophys. Un., 1939, 518–523, 1939.

PAGES 2k Consortium: Continental-scale temperature variability during the past two millennia, Nat. Geosci., 6, 339–346, 2013.

Schulz, M., Mudelsee, M.: REDFIT: estimating red-noise spectra directly from unevenly spaced paleoclimatic time series, Comput. Geosci., 28, 421–426, 2002.

Shi, F., Yang, B., and Von Gunten, L.: Preliminary multiproxy surface air temperature field reconstruction for China over the past millennium, Sci. China Ser. D, 55, 2058–2067, 2012.

Tan, L., Cai, Y., Cheng, H., An, Z., and Edwards, R. L.: Summer monsoon precipitation variations in central China over the past 750 years derived from a high-resolution absolute-dated stalagmite, Palaeogeogr. Palaeocl., 280, 432–439, 2009.

Thorrold, S. R., Campana, S. E., Johns, C. M., and Swart, P. K.: Factors determining $\delta^{13}C$ and $\delta^{18}O$ fractionation in aragonitic otoliths of marine fish, Geochim. Cosmochim. Ac., 61, 2909–2919, 1997.

Wan, N.-J., Li, H.-C., Liu, Z.-Q., and Yuan, D.-X.: Spatial variations of monsoonal rain in eastern China: instrumental, historic and speleothem records, J. Asian Earth Sci., 40, 1139–1150, 2011.

Wang, B.: The Asian Monsoon, Springer Praxis Publishing, Chichester, UK, 787 pp., ISBN: 3-540-40610-7, 2006.

Wang, S., Wen, X., Luo, Y., Dong, W., Zhao, Z., and Yang, B.: Reconstruction of temperature series of China for the last 1000 years, Chinese Sci. Bull., 52, 3272–3280, 2007.

Wang, Y. J., Cheng, H., Edwards, R. L., He, Y., Kong, X., An, Z., Wu, J., Kelly, M. J., Dykoski, C. A., and Li, X.: The Holocene Asian monsoon: links to solar changes and North Atlantic climate, Science, 308, 854–857, 2005.

Wang, Y. J., Cheng, H., Edwards, R. L., Kong, X., Shao, X., Chen, S., Wu, J., Jiang, X., Wang, X., and An, Z.: Millennial- and orbital-scale changes in the East Asian monsoon over the past 224,000 years, Nature, 451, 1090–1093, 2008.

CPD
10, 1305–1335, 2014

Wang, Y. J., Cheng, H., Edwards, R. L., An, Z. S., Wu, J. Y., Shen, C.-C., and Dorale, J. A.: A high-resolution absolute-dated late Pleistocene monsoon record from Hulu Cave, China, Science, 294, 2345–2348, 2001.

Zhang, D. E.: Severe drought events as revealed in the climate records of China and their temperature situations over the last 1000 years, Acta Meteorol. Sin., 19, 485–491, 2005.

Zhang, D. E., Li, X. Q., and Liang, Y. Y.: Continuation (1992–2000) of the yearly charts of dryness/wetness in China for the last 500 years period, J. Appl. Meteorol. Sci., 14, 379–388, 2003 (in Chinese).

Zhang, H.-L., Yu, K.-F., Zhao, J.-X., Feng, Y.-X., Yu-Shi Lin, Y.-S., Zhou, W., and Liu, G.-H.: East Asian summer monsoon variations in the past 12.5 ka: high-resolution δ^{18}O record from a precisely dated aragonite stalagmite in central China, J. Asian Earth Sci., 73, 162–175, 2013.

Zhang, P., Cheng, H., Edwards, R. L., Chen, F., Wang, Y., Yang, X., Liu, J., Tan, M., Wang, X., Liu, J., An, C., Dai, Z., Zhou, J., Zhang, D., Jia, J., Jin, L., and Johnson, K. R.: A test of climate, sun, and culture relationships from an 1810-year Chinese cave record, Science, 322, 940–942, 2008.

CPD

10, 1305–1335, 2014

Table 1. ^{230}Th dating results of stalagmite LHD1.

Depth (mm)	^{238}U (ppb)	^{232}Th (ppt)	$^{230}Th/^{232}Th$ (atomic $\times 10^{-6}$)	$\delta^{234}U^{a}$ (measured)	$^{230}Th/^{238}U$ (activity)	^{230}Th Age (year) (uncorrected)	^{230}Th Age (year) (corrected)	$\delta^{234}U_{Initial}{}^{b}$ (corrected)	^{230}Th Age (year BP) (corrected)
6	3649 ± 8	3471 ± 70	30 ± 1	698 ± 3	0.0017 ± 0.0000	111 ± 1	94 ± 12	698 ± 3	**33 ± 12**
10	4241 ± 8	9600 ± 193	20 ± 1	692 ± 3	0.0028 ± 0.0001	181 ± 3	142 ± 28	693 ± 3	**80 ± 28**
16	3242 ± 5	6847 ± 137	41 ± 1	691 ± 3	0.0052 ± 0.0001	338 ± 7	302 ± 27	692 ± 3	**240 ± 27**
26	5207 ± 6	135 ± 3	4175 ± 100	694 ± 2	0.0066 ± 0.0000	425 ± 3	424 ± 3	695 ± 2	**361 ± 3**
30	4089 ± 8	1891 ± 38	260 ± 6	692 ± 3	0.0073 ± 0.0001	472 ± 5	464 ± 8	693 ± 3	**402 ± 8**
40	4573 ± 6	32 ± 2	20 272 ± 1057	698 ± 2	0.0087 ± 0.0000	557 ± 3	557 ± 3	699 ± 2	**494 ± 3**
55	4224 ± 5	107 ± 3	7210 ± 188	690 ± 2	0.0111 ± 0.0000	715 ± 3	715 ± 3	692 ± 2	**652 ± 3**
70	4532 ± 8	930 ± 19	1030 ± 22	685 ± 3	0.0128 ± 0.0001	832 ± 5	828 ± 5	687 ± 3	**766 ± 5**
90	5509 ± 7	259 ± 5	5537 ± 117	689 ± 2	0.0158 ± 0.0001	1022 ± 4	1022 ± 4	691 ± 2	959 ± 4
109	2803 ± 3	1404 ± 28	612 ± 12	692 ± 2	0.0186 ± 0.0001	1205 ± 4	1196 ± 7	694 ± 2	**1135 ± 7**
118.5	5369 ± 7	141 ± 3	12 936 ± 284	686 ± 2	0.0206 ± 0.0001	1343 ± 5	1343 ± 5	688 ± 2	**1280 ± 5**
125	6011 ± 14	2570 ± 52	860 ± 18	685 ± 3	0.0223 ± 0.0001	1452 ± 7	1445 ± 9	687 ± 3	**1383 ± 9**
140	5430 ± 7	224 ± 5	9899 ± 222	682 ± 2	0.0248 ± 0.0001	1615 ± 6	1615 ± 6	686 ± 2	**1552 ± 6**
149	4100 ± 11	2442 ± 49	714 ± 14	677 ± 3	0.0258 ± 0.0001	1688 ± 7	1678 ± 10	680 ± 3	**1617 ± 10**
170	6060 ± 13	2922 ± 59	952 ± 19	678 ± 3	0.0278 ± 0.0001	1822 ± 7	1814 ± 9	682 ± 3	**1752 ± 9**
175	4190 ± 5	471 ± 10	4097 ± 85	677 ± 2	0.0280 ± 0.0001	1831 ± 7	1829 ± 7	681 ± 2	**1766 ± 7**
185	3757 ± 5	19 ± 7	95 826 ± 38 450	675 ± 2	0.0287 ± 0.0001	1882 ± 7	1882 ± 7	679 ± 2	**1819 ± 7**
195	3047 ± 4	148 ± 3	10 099 ± 221	666 ± 2	0.0298 ± 0.0001	1966 ± 8	1965 ± 8	669 ± 2	**1902 ± 8**
210	4921 ± 11	497 ± 10	5218 ± 108	659 ± 3	0.0319 ± 0.0001	2118 ± 9	2116 ± 9	663 ± 3	**2054 ± 9**
230	3051 ± 4	19 ± 3	88 934 ± 14 365	660 ± 2	0.0341 ± 0.0001	2263 ± 8	2263 ± 8	664 ± 2	**2200 ± 8**
250	4442 ± 7	27 ± 2	98 544 ± 6107	652 ± 2	0.0364 ± 0.0001	2428 ± 7	2428 ± 7	657 ± 2	**2365 ± 7**
260	646 ± 1	535 ± 11	778 ± 17	667 ± 3	0.0391 ± 0.0003	2584 ± 19	2570 ± 22	672 ± 3	**2508 ± 22**
280	2954 ± 5	73 ± 2	27 899 ± 759	674 ± 2	0.0419 ± 0.0001	2762 ± 9	2761 ± 9	679 ± 2	**2689 ± 9**
302	1185 ± 2	2556 ± 51	346 ± 7	665 ± 2	0.0452 ± 0.0001	2999 ± 10	2961 ± 28	671 ± 3	**2900 ± 28**
320	3580 ± 6	9379 ± 188	296 ± 6	531 ± 3	0.0471 ± 0.0002	3403 ± 13	3353 ± 37	536 ± 3	**3291 ± 37**

U decay constants: $\lambda_{238} = 1.55125 \times 10^{-10}$ (Jaffey et al., 1971) and $\lambda_{234} = 2.82206 \times 10^{-6}$ (Cheng et al., 2013). Th decay constant: $\lambda_{230} = 9.1705 \times 10^{-6}$ (Cheng et al., 2013). The error is 2σ error.

[a] $\delta^{234}U = ([^{234}U/^{238}U]_{activity} - 1) \times 1000$.

[b] $\delta^{234}U_{initial}$ was calculated based on ^{230}Th age (T), i.e., $\delta^{234}U_{initial} = \delta^{234}U_{measured} \times e^{\lambda 234 \times T}$.

Corrected ^{230}Th ages assume the initial $^{230}Th/^{232}Th$ atomic ratio of $4.4 \pm 2.2 \times 10^{-6}$. Those are the values for a material at secular equilibrium, with the bulk earth $^{232}Th/^{238}U$ value of 3.8. The errors are arbitrarily assumed to be 50 %. BP stands for "Before Present" where the "Present" is defined as the year 1950 AD.

CPD

10, 1305–1335, 2014

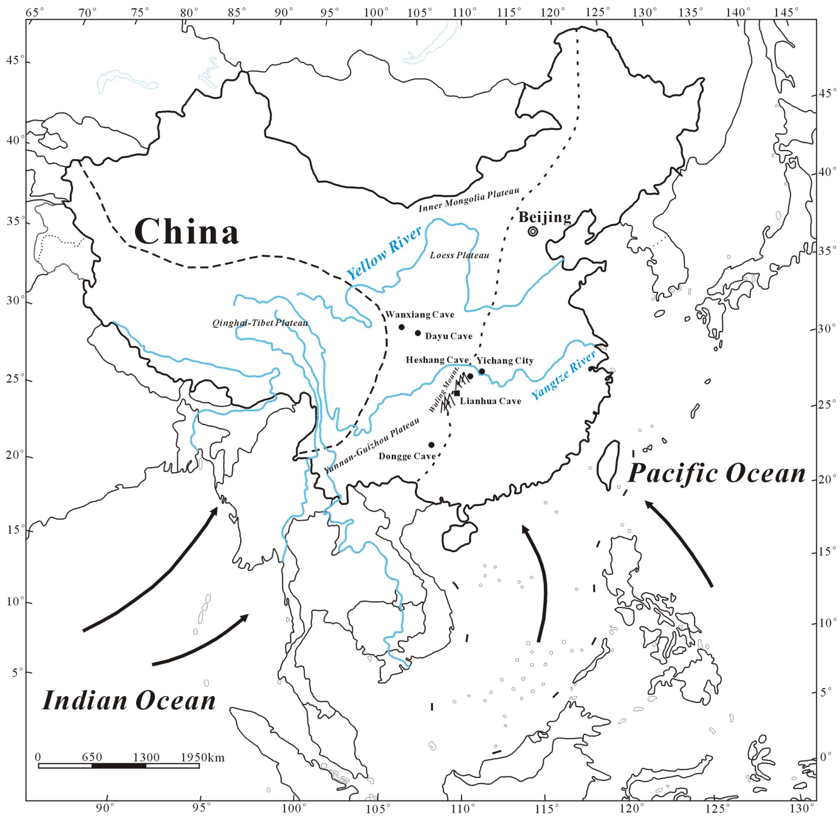

Fig. 1. The location of Lianhua Cave. Long-dashed line stands for the boundary of the Qinghai-Tibet plateau in China. Short-dashed line stands for the boundary of the lower plateau and plain in Eastern China. Wuling Mountain is located at the boundary between Yunnan-Guizhou plateau and Eastern plain. Lianhua cave sits in Wuling mountain. The arrows denote the direction of water vapor flow.

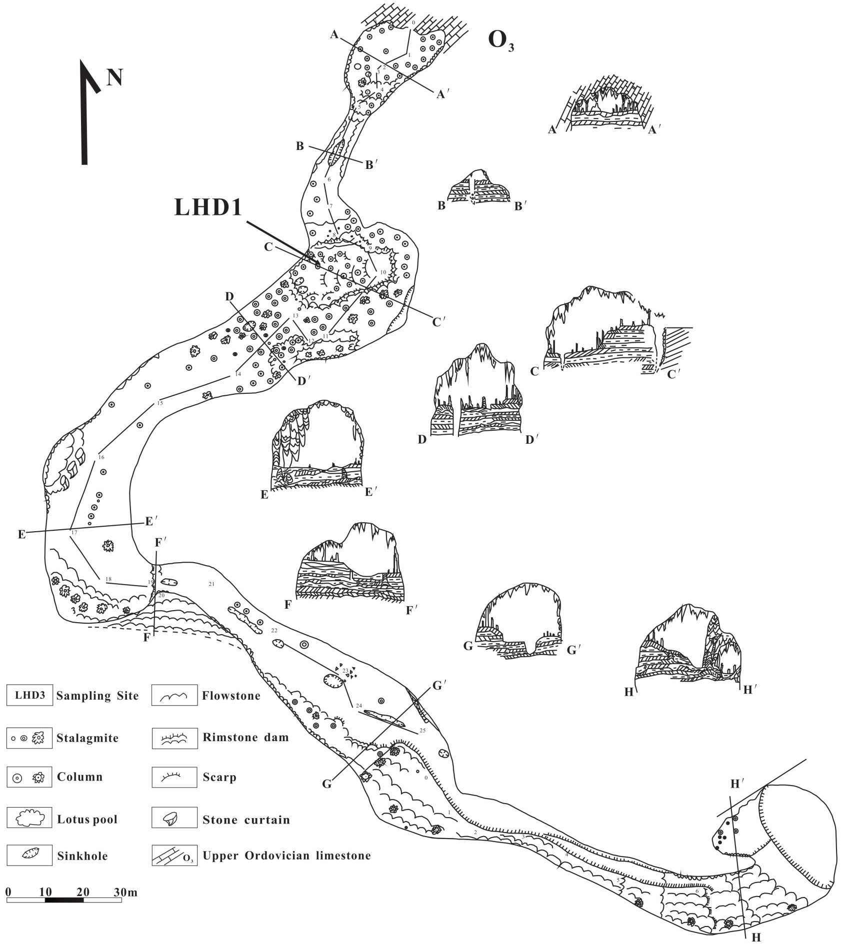

Fig. 2. Schematic map of Lianhua Cave. Stalagmite sample LHD1 was collected in the second chamber.

CPD
10, 1305–1335, 2014

Little Ice Age in central China

J.-J. Yin et al.

Title Page
Abstract
Introduction
Conclusions
References
Tables
Figures
◀
▶
Back
Close
Full Screen / Esc
Printer-friendly Version
Interactive Discussion

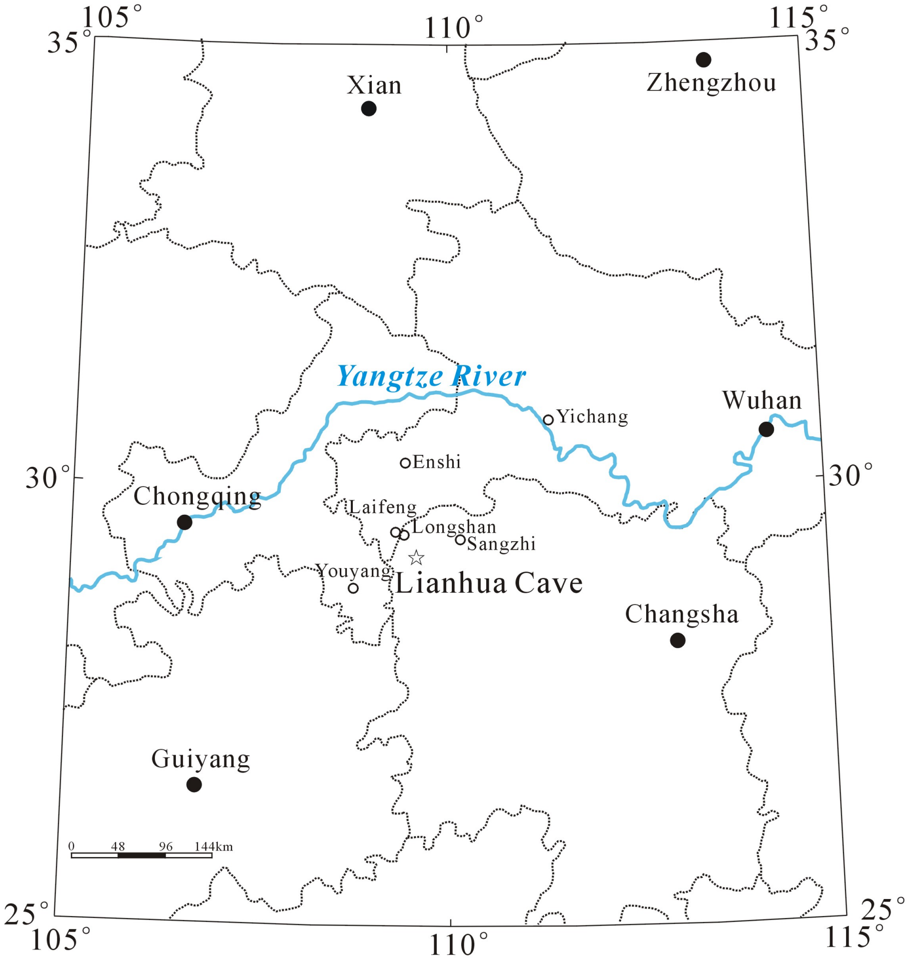

Fig. 3. Meteorological Stations in and around Wuling mountain. The star symbol indicaqtes the location of Lianhua Cave.

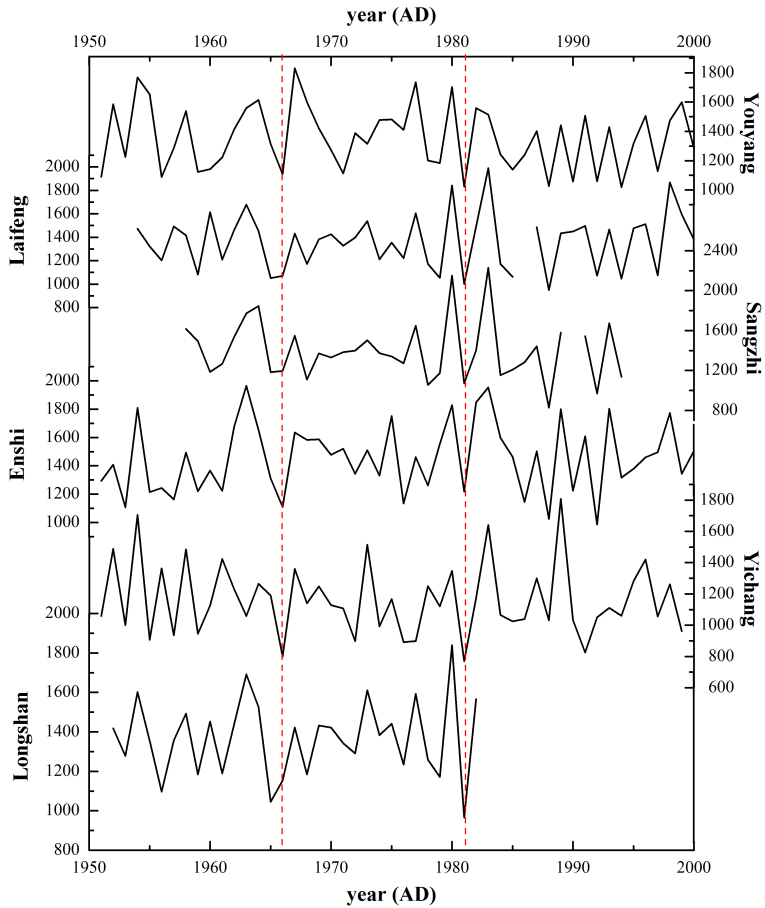

Fig. 4. Precipitation recorded by Meteorological Stations around Lianhua Cave. Red short-dashed lines showed two precipitation plunges occurred during 1965–66 and 1982–83 when strong El Niño occurred.

CPD
10, 1305–1335, 2014

Little Ice Age in central China

J.-J. Yin et al.

Title Page
Abstract
Introduction
Conclusions
References
Tables
Figures
◀
▶
Back
Close
Full Screen / Esc
Printer-friendly Version
Interactive Discussion

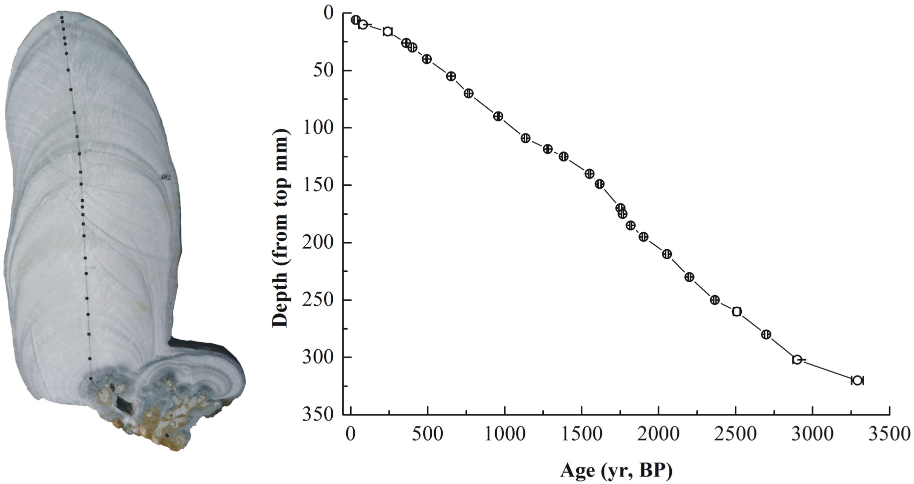

Fig. 5. Photo and age model of stalagmite LHD1. Linear interpolations between two adjacent ^{230}Th dates were used.

CPD
10, 1305–1335, 2014

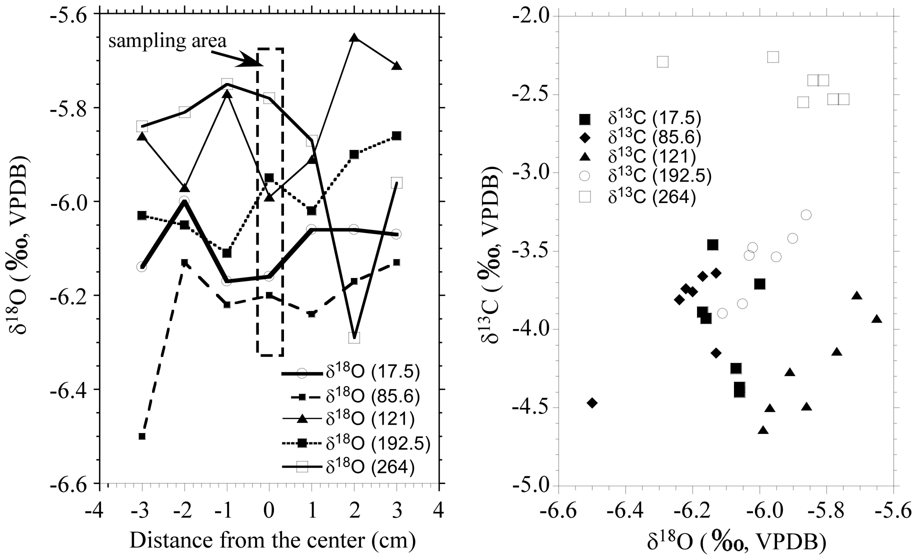

Fig. 6. The results of Hendy Test on five layers of Stalagmite LHD1. **(a)** The $\delta^{18}O$ variation of seven samples along each layer. **(b)** The $\delta^{18}O$ and $\delta^{13}C$ correlations of each layer.

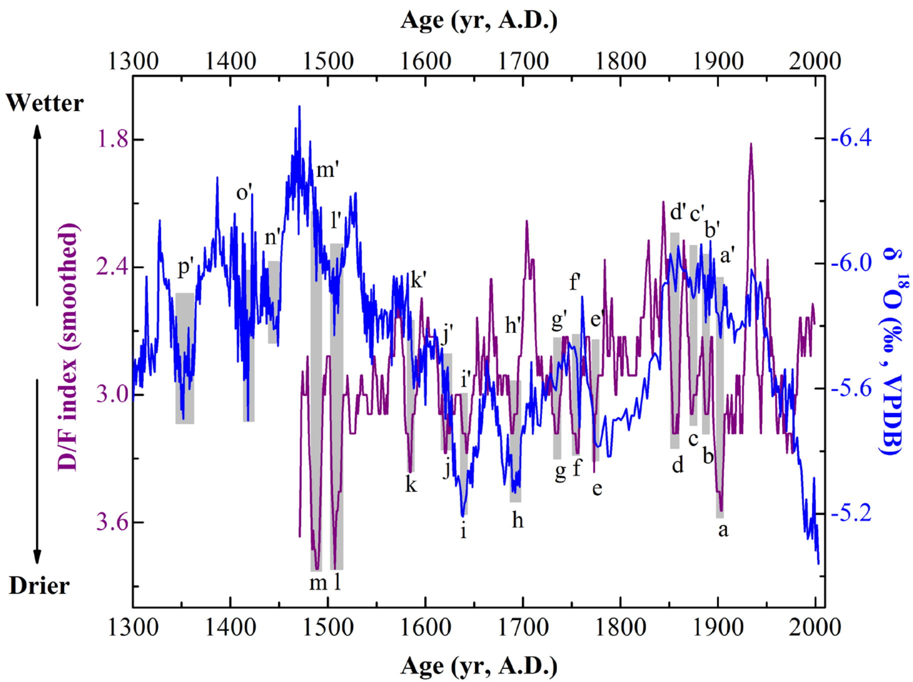

Fig. 7. The δ^{18}O record of Stalagmite LHD1 (blue line), and its comparison with Drought/Flood Index of Yichang City (purple line) (CAMS, 1981) (11 years smoothed). Grey bars and the letters were the drought events found in both records.

CPD
10, 1305–1335, 2014

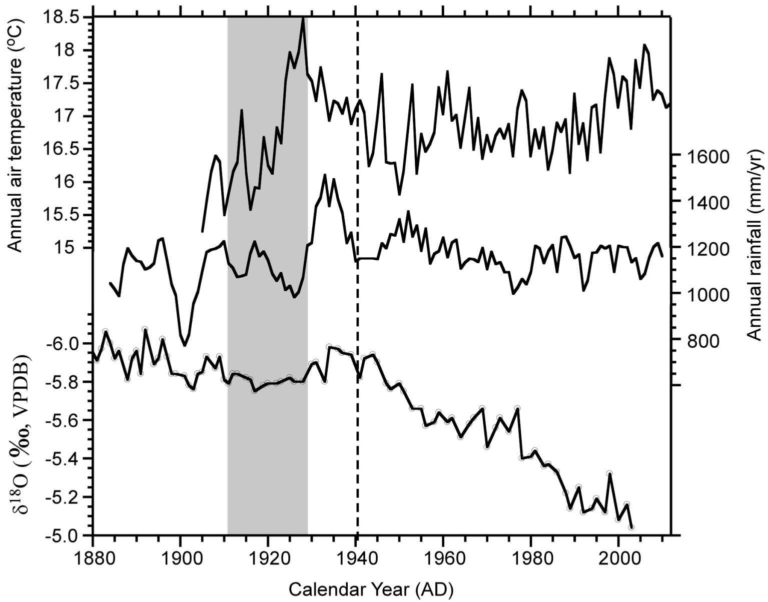

Fig. 8. Comparison of Stalagmite LHD1 δ^{18}O record with the instrumental weather records of Yichang City. The temperature and rainfall records are 5 year running average. The grey bar denotes a period that had opposite trends of temperature and rainfall. The dashed line indicates the beginning of Stalagmite δ^{18}O anomaly.

CPD
10, 1305–1335, 2014

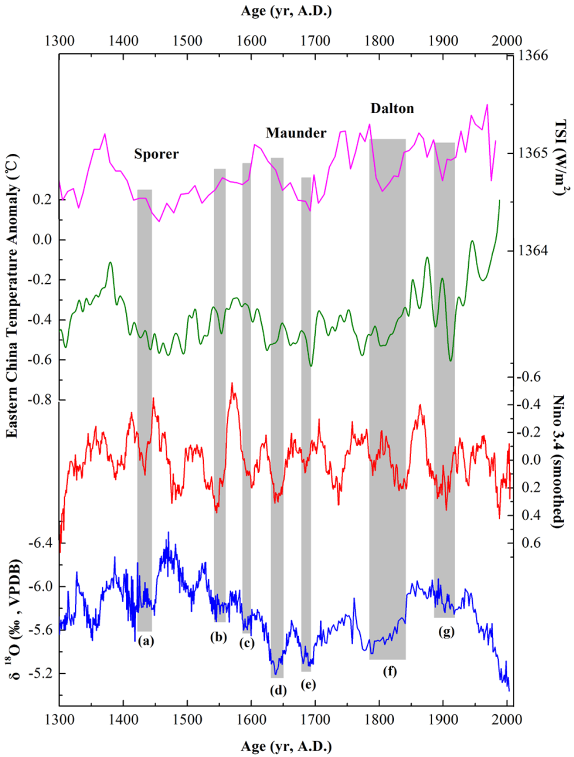

Fig. 9. Comparison of δ^{18}O of Stalagmite LHD1 (blue line) with Total Solar Irradiation (purple line) (Delaygue and Bard, 2011), Eastern China temperature (green line) (Shi et al., 2012), and Niño 3.4 index (red line) (20 years smoothed) (Cook et al., 2008). The grey bars were drought events found in stalagmite LHD1.

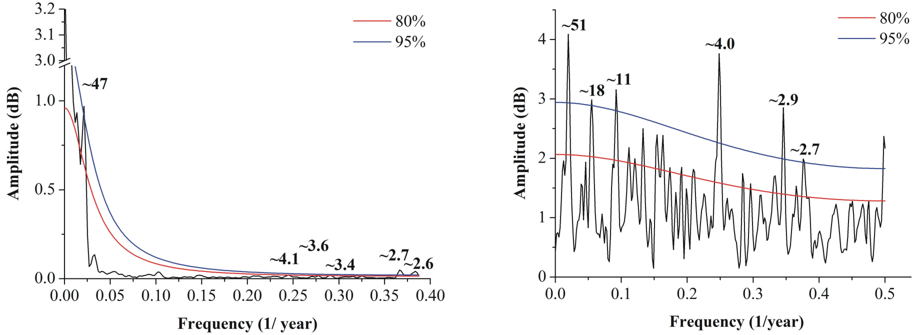

Fig. 10. Spectrum analysis of Stalagmite LHD1 $\delta^{18}O$ record (left) and Niño 3.4 index (right).

CPD
10, 1305–1335, 2014

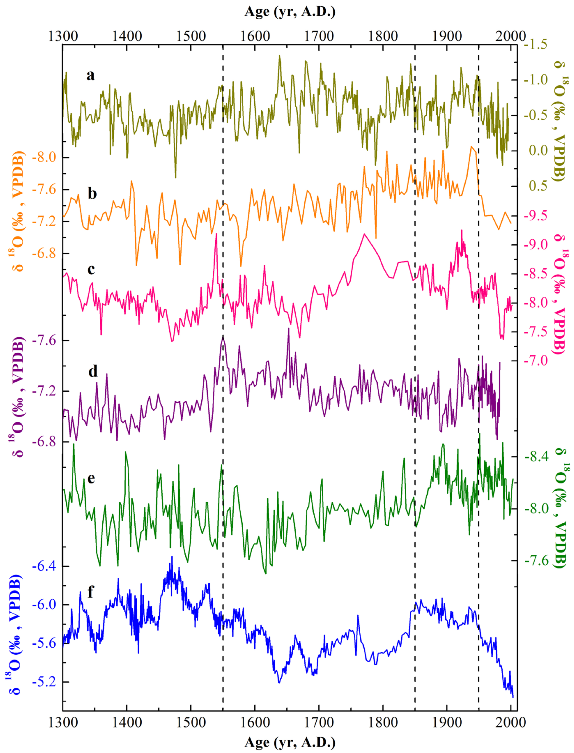

Fig. 11. Comparison of δ^{18}O record of Stalagmite LHD1 with other speleothem records in the Asian monsoonal region. **(a)** S3 record from Defore Cave, Oman, **(b)** DA record from Dongge Cave, China, **(c)** HS-4 record from Heshang Cave, China, **(d)** DY-1 record from Dayu Cave, China, **(e)** WX42B record from Wanxiang Cave, China, and **(f)** LHD1 record (this study). The locations of these Chinese caves were marked in Fig. 1.

CPD
10, 1305–1335, 2014